Global and Planetary Change 244 (2025) 104636

Contents lists available at ScienceDirect

Global and Planetary Change

journal homepage: www.elsevier.com/locate/gloplacha

Response of atmospheric CO_2 changes to the Abyssal Pacific overturning during the last glacial cycle

Yanan Zhang [a], Gang Li [b,c,*], Jimin Yu [d,e], Yi Zhong [a,c], Jianghui Du [f], Xun Gong [g,h], Xiaodong Jiang [i], Congcong Gai [a], Shiying Li [j], Qingsong Liu [a,c,k,*]

[a] Centre for Marine Magnetism (CM²), Department of Ocean Science and Engineering, Southern University of Science and Technology, Shenzhen, China
[b] Key Laboratory of Ocean and Marginal Sea Geology, South China Sea Institute of Oceanology, Chinese Academy of Sciences, Guangzhou, China
[c] Southern Marine Science and Engineering Guangdong Laboratory (Guangzhou), Guangzhou, China
[d] Laoshan Laboratory, Qingdao, China
[e] Research School of Earth Sciences, The Australian National University, Canberra, Australian Capital Territory, Australia
[f] Institute of Geochemistry and Petrology, Department of Earth Sciences, ETH Zürich, Zürich, Switzerland
[g] Hubei Key Laboratory of Marine Geological Resources, China University of Geosciences, Wuhan, China
[h] Shandong Province Key Laboratory of Computer Networks, Qilu University of Technology (Shandong Academy of Sciences), Jinan, China
[i] School of Environmental Science and Engineering, Guangdong University of Technology, Guangzhou, China
[j] Guangdong Marine Geological Survey, Guangzhou, China
[k] Shanghai Sheshan National Geophysical Observatory, Shanghai, China

ARTICLE INFO

Editor: Dr. Jimin Sun

Keywords:
Abyssal Pacific overturning
Oxygenation history
Benthic $\delta^{13}C$
Global carbon cycle
Last glacial cycle

ABSTRACT

Despite its critical role in regulating the global climate and carbon cycle, the evolution of deep Pacific circulation has not been fully deciphered during the last glacial cycle. The effect of deep Pacific hydrographic change (e.g. oxygenation and circulation) on atmospheric CO_2 variation is still uncertain. Here, we study redox-sensitive elements including V-U-Mn and benthic foraminiferal $\delta^{13}C$ at the HYIV2015-B9 site in the southern South China Sea (SCS) to reconstruct the oxygenation and $\delta^{13}C$ signals of water masses during the last glacial cycle. The intra-basin benthic foraminiferal $\delta^{13}C$ gradient suggests enhanced stratification of the deep Pacific during the glacial compared to the interglacial, implying sluggish abyssal Pacific overturning. This is consistent with weak Pacific Deep Water (PDW) ventilation, as indicated by high contents of authigenic V and U, and low authigenic Mn. The inferred sluggish abyssal Pacific overturning is probably associated with less transport of Lower Circumpolar Deep Water, facilitating the expansion of respired carbon storage in the glacial deep Pacific. Meanwhile, the atmospheric CO_2 rise is closely related to active abyssal Pacific overturning since late MIS 5, particularly when considering the impact of Southern Ocean upwelling modulated by Earth's obliquity. Overall, our data indicate the critical role of abyssal Pacific overturning in the carbon cycle, revealing the potential pathway for deep carbon dioxide outgassing in the North Pacific.

1. Introduction

The ocean has been regarded as a primary candidate for regulating atmospheric carbon dioxide (CO_2) during the late Pleistocene glacial cycles, for its huge carbon storage capacity (Sigman and Boyle, 2000; Sigman et al., 2010). Unlike the carbon uptake that occurs in the surface ocean via biological and solubility pumps, ocean circulation plays a crucial role in connecting deep ocean carbon storage to the atmosphere. The transport of carbon-rich deep waters into the surface water increases CO_2 partial pressures, leading to CO_2 outgassing as a consequence (Anderson et al., 2009; Ai et al., 2020; Burke and Robinson, 2012; Sigman et al., 2010).

In contrast to the North Atlantic, the modern North Pacific lacks deep water formation (Warren, 1983). Instead, the deep Pacific basin is occupied by southern-sourced Lower Circumpolar Deep Water (LCDW) through upwelling and diffusion (Kawabe and Fujio, 2010; Talley, 2013). Pacific Deep Water (PDW), the oldest water in the global ocean, contains a large amount of dissolved inorganic carbon (Anderson et al., 2019; Broecker et al., 2004) and is thought to become more carbon enriched during glacials (Jacobel et al., 2017, 2020). The re-surfacing of

* Corresponding authors at: Southern University of Science and Technology, Shenzhen, China; South China Sea Institute of Oceanology, Guangzhou, China.
E-mail addresses: gangli@scsio.ac.cn (G. Li), qsliu@sustech.edu.cn (Q. Liu).

https://doi.org/10.1016/j.gloplacha.2024.104636
Received 1 November 2023; Received in revised form 10 November 2024; Accepted 13 November 2024
Available online 17 November 2024

carbon-rich deep waters could critically affect atmospheric CO_2 on various timescales. Widespread Southern Ocean (SO) upwelling is deemed as the prevailing view for the past rises of atmospheric CO_2 (Anderson et al., 2009; Burke and Robinson, 2012; Sigman et al., 2010). Weakened upwelling would cause the accumulation of respired carbon (Clementi and Sikes, 2017; Ronge et al., 2016; Sikes et al., 2023) accompanied by oxygen consumption (Anderson et al., 2019; Jaccard et al., 2016) through the remineralization of organic matter in the deep ocean. Recent studies suggest that deep carbon storage and atmospheric CO_2 are modulated by multiple ocean regions, rather than solely by the Southern Ocean (Bauska et al., 2021; Rae et al., 2018; Yu et al., 2023). The North Pacific has been suggested to be an important outgassing region of CO_2 that contributed to the atmospheric CO_2 rise during the last deglaciation (Gray et al., 2018; Rae et al., 2014). However, reconstructions of deep Pacific circulation are scarce and existing data sometimes yield conflicting results. The existence of a sluggish/strong deep Pacific circulation that could account for increased/reduced deep Pacific carbon storage during glacial-interglacial cycles is strongly debated (Du et al., 2018; Hall et al., 2001; Hu and Piotrowski, 2018; Rafter et al., 2022). Despite the current two contrasting views of deep Pacific overturning (i.e. the depth of deep Pacific overturning) (Holzer et al., 2021; Stewart, 2017; Talley, 2013), previous models mainly link deep Pacific ventilation to changes in SO upwelling (Menviel et al., 2015; Menviel et al., 2018), neglecting the roles of diffusion in the abyssal Pacific. Besides, ventilation records based on oxygen content are influenced by air-sea disequilibrium at deep water formation regions in cold polar oceans, which complicates assessing impacts from ocean circulation change (Cliff et al., 2021; Dai et al., 2022; Galbraith and Skinner, 2020; Khatiwala et al., 2019). At present, poor constraints on deep Pacific circulation history limits our understanding of the roles of Pacific processes in regulating deep carbon reservoirs and atmospheric pCO_2 fluctuations on glacial-interglacial timescales.

The South China Sea (SCS), as one of the largest marginal seas in the Western Pacific, is well connected to the open Pacific via the only deep passage, the Luzon Strait (~2400 m). Due to the persistent baroclinic pressure gradient, SCS Deep Water (SCSDW) is replenished by an overflow of modern PDW below 1500 m (Qu et al., 2006), leading to similarities in physical-chemical properties between the deep SCS and Pacific (Qu et al., 2006; Wang et al., 2011; Wu et al., 2015). Additionally, the stable sedimentation environment and excellent preservation of carbonate fossils in SCS provide ideal conditions for recording information about past Pacific chemistry changes.

Here we present new benthic foraminiferal $\delta^{13}C$ and high-resolution redox-sensitive elemental data from the southern SCS, to reconstruct the oxygenation history and $\delta^{13}C$ variations of the SCS and PDW. We infer deep ocean water mass structure and PDW ventilation conditions over the past ~90 ka by using the $\delta^{13}C$ spatial gradient and oxygenation records in the deep Pacific. Our data indicate enhanced deep stratification, associated with a sluggish abyssal Pacific overturning, and weak PDW ventilation during marine isotope stage (MIS) 2 and 4. In contrast, strengthened abyssal Pacific overturning reduces ocean stratification and probably assists PDW ventilation during MIS 1, 3, and late MIS 5. This inferred abyssal overturning is closely related to atmospheric CO_2 fluctuations, especially during early MIS 3 and MIS 4, periods when atmospheric CO_2 variations show a weak correlation with SO upwelling. Our new results emphasize the impact of abyssal Pacific overturning on the carbon cycle and indicate a potential pathway for transporting deep Pacific carbon to the atmosphere. Our results highlight that North Pacific processes must be considered to gain a more comprehensive understanding of past atmospheric pCO_2 change.

2. Materials and methods

2.1. Materials

Samples used for this study are obtained from core HYIV2015-B9 (hereafter refer to B9; 10.2484°N, 112.7325°E; 2603 m water depth; bathed in SCSDW), retrieved in the southern SCS during cruise HYIV20150816 of *R/V Haiyang* IV in 2015 (Fig. 1). The core is 4.51 m long and dominated by homogenous gray-dark clay without visible disturbance. The stable sedimentary environment (average deposition rate: ~5.1 cm/kyr) (Zhong et al., 2021) provides a valuable record of SCSDW evolution. The age model has been established by planktonic foraminiferal AMS ^{14}C data (Li et al., 2018) and benthic foraminiferal $\delta^{18}O$ (Zhong et al., 2021). The sedimentary records from this core extend back to late MIS 5 (~ 88.2 ka).

2.2. Methods

In this study, samples were taken at 2–4 cm intervals for stable isotopic and geochemical measurements. Epibenthic foraminifera *Cibicidoides wuellerstorfi* (>150 μm) were picked for stable carbon isotope measurements, which are widely thought to be in equilibrium with $\delta^{13}C$ of ambient seawater (Duplessy et al., 1984; Mackensen, 2012). Foraminiferal $\delta^{18}O$ and $\delta^{13}C$ data were measured on Thermo-Finnigan MAT 253 plus mass spectrometer at Xi'an Jiaotong University in Xi'an, China. All data were calibrated into the international standard Pee Dee Belemnite (PDB). The standard deviations were ± 0.06 ‰ for $\delta^{18}O$ and ± 0.04 ‰ for $\delta^{13}C$.

Differences in $\delta^{13}C$ and [CO2–3] between water masses can be used to reveal the ocean structure and stratification associated with ocean circulation (Hodell et al., 2003; McCave et al., 2008; Ronge et al., 2015; Yu et al., 2014). In this study, sites bathed in LCDW, PDW, and SCSDW have been compiled respectively to analyze the gradients of deep water $\delta^{13}C$ over the last glacial cycle (Fig. 1 and Table S1). To avoid the impact of local factors (e.g. productivity), we compiled $\delta^{13}C$ data from several sites according to water masses to produce regional stacked $\delta^{13}C$ (Fig. S1). Notably, our adopted $\delta^{13}C$ records are derived from *C. wuellerstorfi* in Pacific-SCS sites. Although deep-water $\delta^{13}C$ records could be obtained using data from other species after some corrections using interspecies offset (Elderfield et al., 2012; McCave et al., 2008), these offsets could have varied on glacial-interglacial timescales which will increase uncertainties of finally obtained deep-water $\delta^{13}C$ records (Gottschalk et al., 2016a; Ronge et al., 2015). Thus, we avoid using $\delta^{13}C$ records based on species other than *C. wuellerstorfi*. Also, we use [CO2–3] records from the equatorial Pacific (Yu et al., 2010, 2013) to calculate the vertical [CO2–3] gradient, which is subsequently employed to reveal water-mass geochemical divides and structure in the deep Pacific.

Major elements of bulk sediments from this core were determined using Thermo-Fisher IRIS II Intrepid XSP inductively coupled plasma optical emission spectrometer (ICP-OES), while trace elements and rare earth elements (REE) were analyzed by inductively coupled plasma mass spectrometry (ICP-MS) using PerkinElmer ELAN 9000 at the Institute of Oceanology, Chinese Academy of Sciences in Qingdao, China. The dissolution procedure was as follows: 0.05 g of sample powder was digested in a sealed Teflon beaker with 0.5 ml HF, 0.5 ml HNO_3, and 1.5 ml HCl on a hot plate (120 °C) for ~12 h. Following heating to dryness, 1 ml HNO_3 and 1 ml H_2O were added, and the beaker was sealed and heated on a hot plate (150 °C) for ~12 h to dissolve the residue. Major and trace elements were analyzed along with internal reference materials (GBW07315, GBW07316, BCR-2, BHVO-2, GBW07296, NOD-P-1, NOD-A-1).

Titanium (Ti) in marine sediments is thought to be mainly derived from terrigenous sources (Goldberg and Arrhenius, 1958; Wei et al., 2003). Hence, authigenic (or biogenic) elements (e.g. U_{auth}, V_{auth}, Ba_{bio}, Mn_{auth}) could be estimated by subtracting the detrital contribution from total concentrations through the following formula (1) (Jaccard et al., 2009; Li et al., 2018) using Ti concentrations. Average elemental concentrations of detrital fraction from adjacent core NS90–103 (Wei et al., 2000) are used to represent the composition of terrigenous fraction in this study.

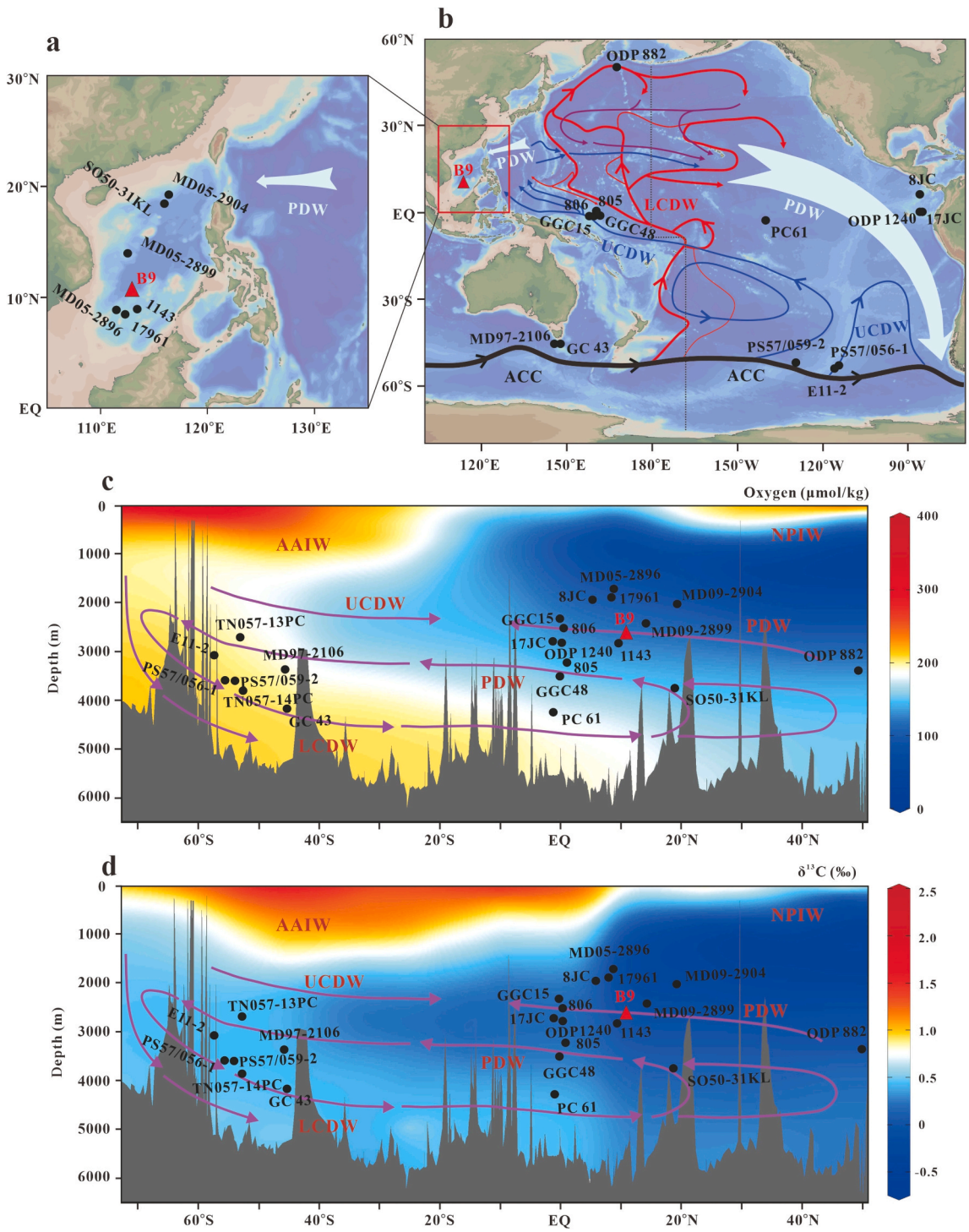

Fig. 1. Core sites and modern Pacific circulation. a. Sediment cores used in this study (HYIV2015-"B9", red triangle) and other sites (black dots) (see Supplementary Table 1). b. Modern deep Pacific circulation from (Kawabe and Fujio, 2010). c and d. Meridional section of dissolved oxygen and $\delta^{13}C$ distribution (the black dotted line in b) based on the GLODAP dataset (Key et al., 2004), and a schematic showing deep Pacific circulation with white arrow lines. ACC: Antarctic Circumpolar Current; LCDW: Lower Circumpolar Deep Water; UCDW: Upper Circumpolar Deep Water; PDW: Pacific Deep Water; NPIW: North Pacific Intermediate Water. Figures produced by Ocean Data View software (Schlitzer, 2022). Information of sediment cores can be found in Table S1. (For interpretation of the references to colour in this figure legend, the reader is referred to the web version of this article.)

$$M_{auth}\ (M_{bio}) = M_{bulk} - Ti_{bulk}{}^{*}M_{detr}/Ti_{detr} \quad (1)$$

where M_{auth} (M_{bio}) is the authigenic or biogenic elements, and M_{total} and Ti_{total} represent the total concentration of elements and Ti in sediments, respectively. The values of M_{detr}/Ti_{detr} are element ratios relative to Ti of terrigenous fraction estimated from core NS90–103 (V_{detr}/Ti_{detr} = 0.0263; $U_{detr}/Ti_{detr} = 6{*}10^{-4}$; Mn_{detr}/Ti_{detr} = 0.12; Ba_{detr}/Ti_{detr} = 0.135) (Wei et al., 2000).

The enrichment of redox-sensitive elements (e.g. V_{auth}, Mn_{auth}, U_{auth}) in marine sediments is primarily influenced by the redox conditions of sediments. This enrichment could be utilized to reconstruct oxygenation histories of sedimentary environments (Jaccard et al., 2016; Loveley

et al., 2017; Marcantonio et al., 2020; Tribovillard et al., 2006; Zou et al., 2020). In well-oxygenated settings, dissolved Mn (II) is typically oxidized to higher oxidation states including Mn(III) and Mn(IV), resulting in the precipitation of relatively insoluble oxyhydroxide and/or oxide (Calvert and Pedersen, 1996; Hawco et al., 2016). Conversely, V and U tend to accumulate as insoluble products in sediments under suboxic-anoxic conditions (Calvert and Pedersen, 1993; Morford and Emerson, 1999). Although V and U exhibit similar behavior, it is believed that the redox threshold for V reductions is higher than for U (Morford and Emerson, 1999; Shaw et al., 1990). Biogenic Ba (Ba_{bio}) concentration, which is delivered to the seafloor as the mineral barite, is closely related to organic matter export (Francois et al., 1995; Paytan et al., 1996; Schoepfer et al., 2015). In non-sulfate-reducing environments, Ba_{bio} has been widely used to reconstruct the export productivity over different geological time scales (Carter et al., 2016; Jaccard et al., 2005; Paytan and Kastner, 1996; Yao et al., 2021).

3. Results

Combined with data from the upper part of core B9 (Li et al., 2018), our benthic $\delta^{13}C$ data extend the record to the late MIS 5, showing a range from 0.23 ‰ to −0.35 ‰. Benthic $\delta^{13}C$ records display high values during warm intervals (about 0.09 ‰ in the Holocene, −0.06 ‰ in MIS 3 and − 0.04 ‰ in late MIS 5), and low values during cold intervals (about −0.2 ‰ in MIS 2 and − 0.3 ‰ in MIS 4) (Fig. 2a). Similar $\delta^{13}C$ records are also observed at other sites that bathed in SCSDW (Fig. S1), revealing a regional change of dissolved inorganic carbon in deep waters. Although benthic $\delta^{13}C$ data in MIS 4 are limited, a noticeable decline can be observed from the late MIS 5 to MIS 4. The magnitude of $\delta^{13}C$ change between the Holocene and LGM is about 0.29 ‰, which is comparable to the change associated the PDW (Lisiecki, 2010; Peterson et al., 2014).

The V_{auth} and U_{auth} concentrations range from 12 to 88 ppm and 0.2 to 2.4 ppm, respectively (Fig. 2). Both V_{auth} and U_{auth} concentrations show high values during cold intervals and low values during warm intervals (Fig. 2b and d). However, V_{auth} enrichment is evident, but U_{auth} is absent in core B9 during MIS 4. Total Mo concentrations are generally lower than 4 ppm (Fig. 2c), showing a subtle enrichment relative to the average PostArchean Australia Shale (1 ppm, Taylor and Mclennan, 1985) or regional detrital composition (~ 0.93 ppm, Wei et al., 2000). The increased concentrations of Mo in the core top samples are probably associated with the co-precipitation of Mn (Calvert and Pedersen, 1993; Nameroff et al., 2002). In contrast to V_{auth} and U_{auth}, Mn_{auth} and Ba_{bio} exhibit opposite trends in core B9, displaying high values during warm intervals and low values during cold intervals (Fig. 2c and e). Elevated contents of TiO_2 in glacial sediments of core B9 were widely found on continental margins, indicating increased terrigenous flux during intervals of low-sea-level (Goldberg and Arrhenius, 1958; Jaccard et al., 2005) (Fig. 2f).

4. Discussion

4.1. Redox-sensitive elements and deep waters oxygenation

After removing detrital signals, authigenic redox elements can reflect the variability of sediment oxygenation conditions (Durand et al., 2018; Jaccard et al., 2009; Li et al., 2018). As mentioned above, authigenic precipitation of V and U would increase, while sedimentary Mn depletes under suboxic conditions. The sedimentary redox conditions should result in anti-correlated changes in V_{auth}/U_{auth} and Mn_{auth}. Consideration of these redox indicators could improve the accuracy of

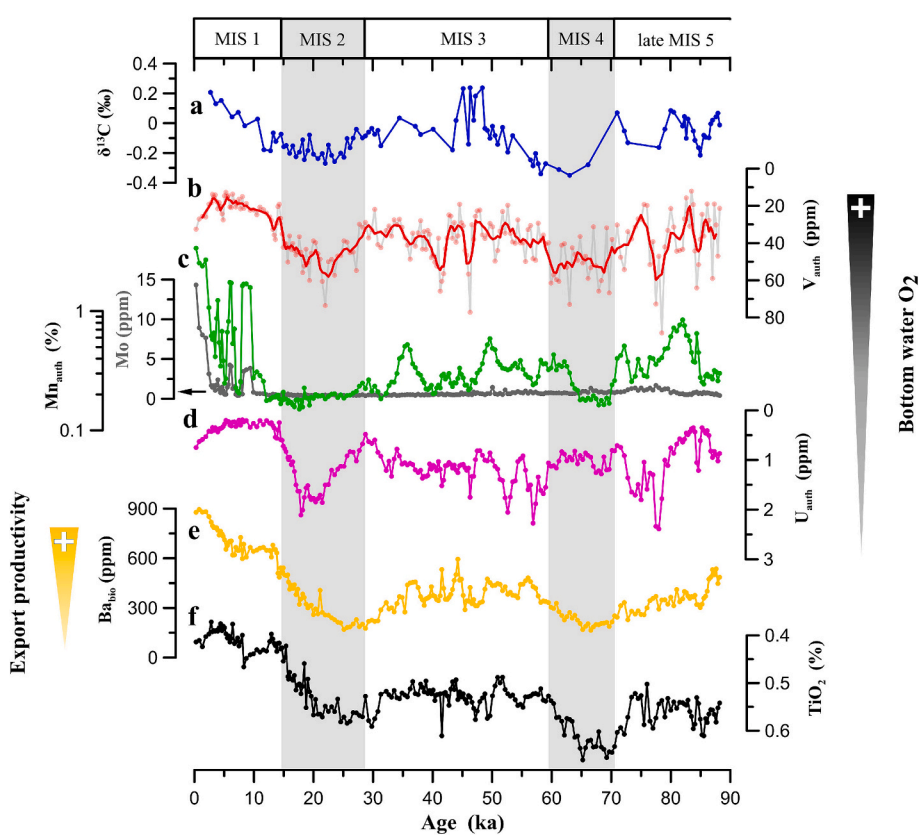

Fig. 2. Paleo-proxy records in core B9. a. $\delta^{13}C$ in *C. wuellerstorfi*, b. The concentrations of authigenic V. c. The concentrations of Mo and authigenic Mn. d. The concentrations of authigenic U. e. Biogenic Ba reflects export productivity. f. TiO_2 relative content indicates terrigenous supply. The five-point moving average of V_{auth} (red line) and raw data (dots). Black arrow indicates average Mo compositions of detrital sediment from NS90–103 in southern South China Sea (Wei et al., 2000). Colour bars denote MIS 2 and 4. (For interpretation of the references to colour in this figure legend, the reader is referred to the web version of this article.)

sedimentary redox conditions. In contrast to the warm periods (MIS 1, 3, and late MIS 5), high V_{auth} and U_{auth} contents coupled with depleted Mn_{auth} occur during cold periods (MIS 2 and 4) (Fig. 2b-d). Potential post-depositional remobilization during renewed pore water O_2 exposure (burn-down) may complicate the interpretations of authigenically precipitated redox elements (Crusius and Thomson, 2000; Jacobel et al., 2017). This process would lead to the removal of authigenic elements in the upper part (e.g. U_{auth}) and the formation of re-immobilization peaks below the O_2 penetration depth, especially where sedimentation rates are <2 cm/kyr (Costa et al., 2018; Jaccard et al., 2009; Mangini et al., 2001). However, the average sedimentation rate at the B9 site is ~5.1 cm/kyr, which helps the preservation of original redox condition signals. Our Mn and Mo results from the same core suggest insignificant transient enrichments that result from post-depositional burn-down (Fig. 2c). Hence, we attribute redox element data at the B9 site to reflect sedimentary redox conditions over the past ~90 ka, which indicate more oxidizing environments during warm periods than those of cold periods.

The interpretation of sedimentary redox conditions require disentanglement of two factors: regional/local organic matter export from the surface ocean and the supply of oxygen in bottom waters (Kumar et al., 1995; McManus et al., 2005; Zheng et al., 2002). Ba_{bio} records from core B9 indicate higher productivity during warm intervals compared to cold intervals (Fig. 2e), consistent with biogenic opal records from nearby core NS93–5 (Chen et al., 2008). The porewater measurement from ODP site 1143 suggests the absence of sulfate-reducing conditions in the study area since the late Pleistocene (SO2–4 > 20 mM) (Shipboard Scientific Party, 2000), excluding the possibility of Ba_{bio} fluctuations due to barite dissolution. This is further evidenced by low Mo contents at our site B9 (Fig. 2c) and supports the utility of Ba_{bio} as an export productivity proxy (Jaccard et al., 2009; Nan et al., 2023). Given the absence of increased biogenic fluxes based on Ba_{bio} during MIS 2 and MIS 4, the observed reducing environments recorded in core B9 cannot be explained by export production changes in the southern SCS. Thus, the redox state of marine sediments, decoupled with export production, is likely controlled by the oxygen level of bottom waters (Jaccard et al., 2016; Jacobel et al., 2017; Loveley et al., 2017). We find similar oxygenation histories between the SCS and the open Pacific, implying that the source of SCSDW has not changed since the late MIS 5 and is well connected with the open Pacific (Fig. 3). The similarity between stacked $\delta^{13}C$ records from the SCS and western equatorial Pacific also supports this view (Fig. 4a), which is further confirmed by [CO2–3] records from the deep SCS (Wan et al., 2020). However, some detailed differences exist between redox condition records, possibly reflecting local factors (e.g., burn-down of U_{auth} in the central equatorial Pacific and productivity changes in the north and eastern equatorial Pacific) (Jaccard et al., 2009; Jacobel et al., 2017, 2020; Loveley et al., 2017). Overall, our redox-sensitive elements records tie well with atmospheric CO_2 records over the past ~90 ka and are independent of the local

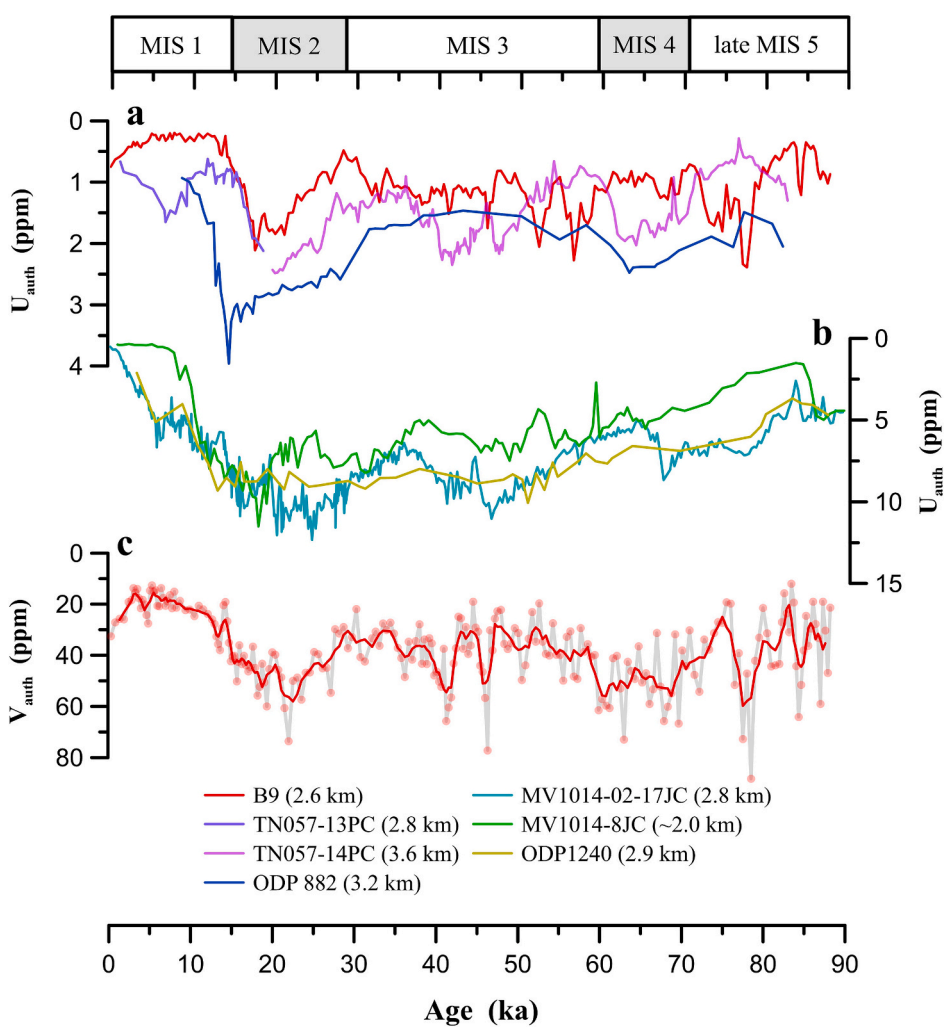

Fig. 3. Records of water masses oxygenation. a and b. U_{auth} records from B9 (this study), open Pacific: ODP 882 (Jaccard et al., 2009); MV1014–02–17JC (Loveley et al., 2017); MV1014-8JC (Marcantonio et al., 2020); ODP 1240 (Jacobel et al., 2020), and TN057–13/14PC (Jaccard et al., 2016) bathed in LCDW. c. V_{auth} records in B9 (this study).

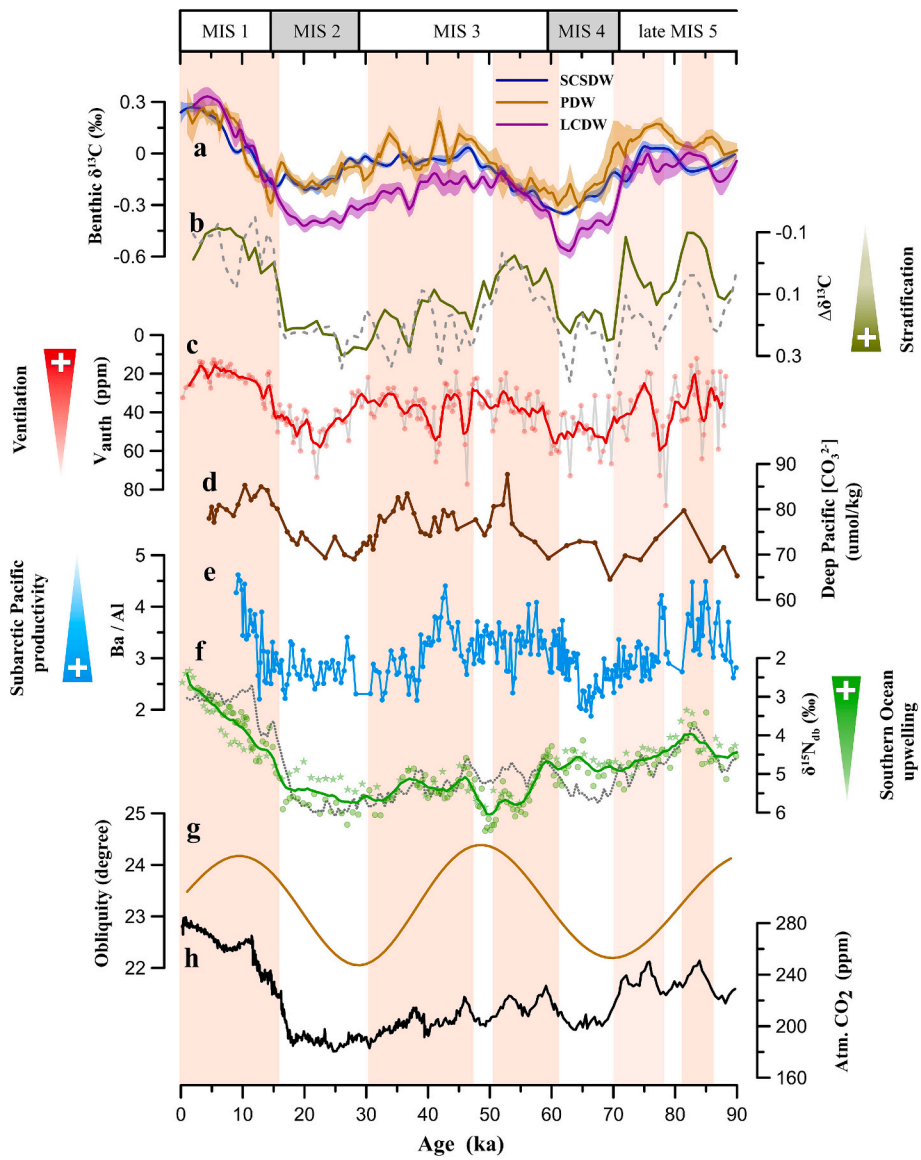

Fig. 4. Variation in Pacific abyssal overturning compared to other processes over the last ~90 ka. a. the stacked $\delta^{13}C$ of SCSDW, PDW and LCDW, respectively (with σ confidence intervals). b. Deep Pacific structure suggests by $\Delta\delta^{13}C_{SCSDW\text{-}LCDW}$ (black green line) and $\Delta\delta^{13}C_{PDW\text{-}LCDW}$ (gray dotted line) (this study). c. Ventilation based on authigenic V concentrations from core B9 (red line is the five-point weighted average and dots are the raw data; this study). d. deep Pacific [CO2–3] derived from B/Ca (Yu et al., 2010, 2013). e. Ba/Al data from ODP 882 (Jaccard et al., 2009). f. Diatom-bound $\delta^{15}N$ that represents the Southern Ocean upwelling (green line: the estimated mean average). Dotted line is the predicted $\delta^{15}N$ from Antarctic temperature. Green dots are data from MD11–3394 and green stars are data from MD12–3353 (Ai et al., 2020). g. Obliquity (Berger and Loutre, 1991). h. Composite atmospheric CO_2 concentration records from Antarctic ice cores (Bereiter et al., 2012). Colour bars represent periods with elevated atmospheric CO_2 concentration. Information of sediment cores can be found in Table S1. (For interpretation of the references to colour in this figure legend, the reader is referred to the web version of this article.)

changes in productivity, suggesting the important roles of PDW ventilation in regulating atmospheric CO_2 (Fig. 4).

4.2. Abyssal Pacific overturning and global carbon cycle

In addition to our redox sensitive indicators, we also employ benthic $\delta^{13}C$ to investigate changes in deep Pacific water overturning circulation. Uncertainties associated with the interpretation of seawater $\delta^{13}C$ (via the benthic foraminifera proxy data) include air-sea exchange and the biological pump in the regions of deep-water formation, as well as local productivity and interior respiration modulated by overturning circulation (Broecker and McGee, 2013; Khatiwala et al., 2019; Lynch-Stieglitz et al., 1995; Schmittner et al., 2013; Sikes et al., 2017). The $\delta^{13}C$ gradient ($\Delta\delta^{13}C$) could indicate the structure of interior water masses through a geochemical divide, which is associated with ocean circulation (McCave et al., 2008; Ronge et al., 2015; Sikes et al., 2016; Yu et al., 2013). Additionally, the absence of an obvious decline in benthic $\delta^{13}C$ in core B9 during high export productivity periods (Fig. 2a and e) suggests that the impact of local productivity on benthic $\delta^{13}C$ is negligible. The $\delta^{13}C$ gradient between SCSDW and LCDW ($\Delta\delta^{13}C_{SCSDW\text{-}LCDW}$) illustrates significant changes in water mass structure in the deep Pacific over the past ~90 ka (Fig. 4a and b). We obtain similar changes from $\delta^{13}C_{PDW\text{-}LCDW}$ because stacked $\delta^{13}C_{PDW}$ exhibits similar variation compared to $\delta^{13}C_{SCSDW}$ (Fig. 4b). Higher values of $\Delta\delta^{13}C_{SCSDW\text{-}LCDW}$/$\Delta\delta^{13}C_{PDW\text{-}LCDW}$ in MIS 2 and 4 mean increased $\delta^{13}C$ differences between LCDW and SCSDW (or PDW). We find that deep water [CO2–3] gradients in the Pacific also generally support enhanced deep stratification from late MIS 5 to MIS 2 (Fig. S2). This is probably associated with a slowdown of abyssal Pacific overturning during glacials, reducing the mixing of those water masses (Du et al., 2018; Rafter et al., 2022). This is

supported by inferred reductions in glacial AABW formation (Huang et al., 2020; Yu et al., 2020). Previous carbon isotope modeling results also support this view, revealing the impact of reduced AABW on carbon sequestration in the deep Pacific and atmospheric $\delta^{13}CO_2$ (Menviel et al., 2015, 2017). As an integrated history of organic carbon remineralization, respired carbon in the deep Pacific is not only associated with the soft tissue biological pump in the Southern Ocean (Gottschalk et al., 2016b; Jaccard et al., 2013; Martínez-García et al., 2014), but also related to changes in transit pathway. Poor PDW ventilation and sluggish abyssal Pacific overturning during MIS 2 and 4 likely lead to accumulation of respired carbon in the deep Pacific through increased residence time of deep waters, despite no increase in productivity across the wider Pacific (Costa et al., 2016; Jacobel et al., 2020; Winckler et al., 2016). This could also contribute to the increase in deep carbon storage (Fig. 4d) and consume dissolved oxygen stoichiometrically, resulting in simultaneously low oxygen concentrations (Jacobel et al., 2017, 2020; Yu et al., 2010, 2013). Although previous studies suggest glacial enhanced ventilation below 3.5 km based on U_{auth} (Hu et al., 2023; Jacobel et al., 2017; Thiagarajan and McManus, 2019), it is difficult to guarantee its preservation under low sediment rates (Jacobel et al., 2020). The sluggish abyssal Pacific overturning likely facilitates carbon sequestration in deep Pacific below 3.5 km during glacial, which is further confirmed by deep Pacific [CO2–3] records (Yu et al., 2013). Notably, our and previous inferences of enhanced respired carbon during glacials based on oxygenation records is potentially influenced by air-sea disequilibrium in the deep water formation area (Cliff et al., 2021; Eggleston and Galbraith, 2018; Khatiwala et al., 2019; Stephens and Keeling, 2000; Stott et al., 2021). However, it is challenging to attribute ocean structural changes suggested by our $\delta^{13}C$ gradient results to air-sea disequilibrium alone (Matsumoto et al., 2002; Rafter et al., 2022). The oxygen concentration mismatch between predictions by the model and paleoceanographic data also indicates the overestimate of air-sea disequilibrium in bottom oxygen (Jacobel et al., 2020). Thus, combined with changes in ocean stratification and oxygenation, we speculate that sluggish abyssal Pacific overturning likely played an important role in deep carbon storage in the past.

Based on our findings, we suggest that abyssal Pacific overturning changes can significantly affect past atmospheric pCO_2. The modeling study by Holzer et al. (2021) demonstrates that vertical diffusion transport in the modern North Pacific could transport carbon-rich deep waters to the surface ocean. The active diapycnal diffusion and mixing would enhance deep ocean ventilation (Holzer et al., 2021; Oka and Niwa, 2013; Talley, 2013). During MIS 1 and late MIS 5, our new data suggest the breakup of deep stratification with enhanced PDW ventilation (Fig. 4b and c). This may cause resurfacing of deep waters through vertical diffusion in the North Pacific, leading to blooms in surface productivity (Fig. 4e) (Jaccard et al., 2005, 2009) and deglacial CO_2 degassing (Gray et al., 2018; Rae et al., 2014). Theoretical arguments suggest that the surface buoyancy forcing in the Southern Ocean, related to sea ice (Antarctic temperature), could directly regulate vertical mixing and stratification in the ocean interior (Ferrari et al., 2014; Jansen and Nadeau, 2016; Jansen, 2016), or even in the North Pacific. This has been confirmed by comparing intermediate and deep εNd records in the North Pacific, showing the active abyssal overturning driven by the Southern Ocean processes (Du et al., 2016, 2018). Meanwhile, the poleward shift of Westerly Winds during the peak of global warmth in the late MIS 5 and MIS 1 would act to strengthen SO upwelling (Ai et al., 2020, 2024; Whittaker et al., 2011), helping the re-surfacing of carbon-rich waters in the Southern Ocean (Anderson et al., 2009; Menviel et al., 2018; Rae et al., 2018; Skinner et al., 2010) and the eastern equatorial Pacific through their subsequent advection (de la Fuente et al., 2015; Martínez-Botí et al., 2015). The breakup of stratification and enhanced upwelling in polar oceans (North and South Pacific) likely contributed to the rise of atmospheric CO_2 during MIS 1 and late MIS 5. However, a recent study reveals that variation in atmospheric pCO_2 becomes decoupled from SO upwelling intensity after the MIS 5-MIS 4 transition (Ai et al., 2020). Instead, atmospheric pCO_2 seems closely related to abyssal Pacific overturning change (Fig. 4). It is hard to explain the contemporary variations of atmospheric CO_2 and deep Pacific carbon storage by SO upwelling alone, which is also impacted by obliquity via the temperature gradient between mid- and high-latitudes (Ai et al., 2020, 2024; Lu et al., 2010; Sachs et al., 2001; Timmermann et al., 2014). During MIS 3 (particularly in ~48–57 ka), high obliquity would have weakened wind-driven upwelling in the Southern Ocean for the decrease of temperature gradient (Fig. 4f-g) (Ai et al., 2020; Whittaker et al., 2011). Increased vertical diffusion (North Pacific) driven by abyssal Pacific overturning may have played a more significant role in the rise of atmospheric CO_2 and deep Pacific ventilation. Opposing situations occur in MIS 4. The expanded deep Pacific carbon storage (Bradtmiller et al., 2010; Jacobel et al., 2017, 2020; Matsumoto et al., 2002; Yu et al., 2013) seems to be closely related to North Pacific stratification (weakened overturning), rather than enhanced SO upwelling (Fig. 4). This is confirmed by previous studies that suggest the Southern Ocean is not the only region of CO_2 outgassing and contributions from other regions (e.g., North Pacific) should also be considered (Bauska et al., 2021; Gray et al., 2018; Yu et al., 2023). Therefore, we surmise the potential existence of a deep carbon dioxide transport pathway in the North Pacific through vertical diffusion during atmospheric pCO_2 rise, especially during early MIS 3. Indeed, the re-surfacing of deep waters in the North Pacific is also influenced by North Pacific Intermediate Water (Gong et al., 2019; Gray et al., 2018; Rae et al., 2014). There is clear need for further study on the exchange between intermediate and deep circulation and its impact on carbon cycling.

In summary, we propose a hypothetical scheme of deep Pacific circulation change since the last glacial cycle. Our results reveal an intensified stratification in the deep Pacific during MIS 2, leading to a significant geochemical division (Adkins et al., 2002; Matsumoto et al., 2002). This could have facilitated carbon sequestration in the deep Pacific and lowered atmospheric pCO_2, in synergy with weakened SO upwelling (Dai et al., 2022; Martínez-García et al., 2014; Sigman et al., 2010). Conversely, increased vertical diffusion transport in the North Pacific and strengthened SO upwelling contributed to the rise in atmospheric pCO_2 during MIS 1 and late MIS 5. More importantly, abyssal Pacific overturning seems to play a more dominant role in driving atmospheric CO_2 during the early MIS 3 and MIS 4 than to SO upwelling. Our results highlight the significant impacts of the North Pacific on past atmospheric pCO_2 variations, which is valuable for interpreting the CO_2 variability recorded in ice cores (Bauska et al., 2021; Marcott et al., 2014).

5. Conclusions

Our new redox-sensitive elements and benthic $\delta^{13}C$ records from the deep SCS provide clues to decipher PDW properties in the past. By examining oxygenation indicators and spatial $\delta^{13}C$ gradients between SCSDW/PDW and LCDW, variations of PDW ventilation and ocean stratification, associated with abyssal Pacific overturning variations, have been reconstructed over the past ~90 ka. Our data suggest that enhanced deep stratification, related to sluggish abyssal overturning, is conducive to enhanced carbon storage and lower oxygen levels in the deep Pacific during MIS 2. Additionally, the North Pacific likely serves as a potential pathway for deep carbon release through enhanced vertical diffusion when deep stratification collapsed during MIS 1, 3, and late MIS 5. These results show the significant impacts of abyssal Pacific overturning on atmospheric pCO_2. Abyssal circulation in the North Pacific must be considered if we are to comprehensively understand carbon release and sequestration on glacial-interglacial timescales.

CRediT authorship contribution statement

Yanan Zhang: Writing – review & editing, Writing – original draft, Visualization, Validation, Methodology, Investigation, Formal analysis,

Data curation, Conceptualization. **Gang Li:** Writing – review & editing, Supervision, Methodology, Investigation, Funding acquisition, Conceptualization. **Jimin Yu:** Writing – review & editing, Methodology, Investigation. **Yi Zhong:** Writing – review & editing, Investigation, Funding acquisition, Formal analysis, Data curation, Conceptualization. **Jianghui Du:** Writing – review & editing, Visualization, Validation, Investigation, Conceptualization. **Xun Gong:** Writing – review & editing, Investigation. **Xiaodong Jiang:** Writing – review & editing, Methodology, Investigation. **Congcong Gai:** Writing – review & editing, Investigation. **Shiying Li:** Writing – original draft, Visualization, Data curation, Conceptualization. **Qingsong Liu:** Writing – review & editing, Writing – original draft, Supervision, Investigation, Funding acquisition.

Declaration of competing interest

The authors declare that they have no known competing financial interests or personal relationships that could have appeared to influence the work reported in this paper.

Data availability

See doi:https://doi.org/10.5281/zenodo.7844250 for the data acquired during this study.

Acknowledgment

We would like to thank all crew of the R/V Haiyang IV of Guangzhou Marine Geological Survey from the 2015 cruise. We thank Zhong Chen, South China Sea Institute of Oceanology, Chinese Academy of Sciences for helpful sampling. We thank Xuan Ji and Weiqi Yao for the data analysis and discussion. Our work is supported by the National Natural Science Foundation of China (42176079, 42261144739, 92158208, 42274094, 41976062, 42330403), National Key Research and Development Program of China (2021YFC3100600), Special Fund of South China Sea Institute of Oceanology of the Chinese Academy of Sciences (SCSIO2023QY05), and State Key Laboratory of Marine Geology, Tongji University (No. MGK202209).

Appendix A. Supplementary data

Supplementary data to this article can be found online at https://doi.org/10.1016/j.gloplacha.2024.104636.

References

Adkins, J.F., Mcintyre, K., Schrag, D.P., 2002. The salinity, temperature, and $\delta^{18}O$ of the Glacial Deep Ocean. Science 298 (5599), 1769–1773. https://doi.org/10.1126/science.1076252.

Ai, X.E., Studer, A.S., Sigman, D.M., Martínez-García, A., Fripiat, F., Thöle, L.M., Michel, E., Gottschalk, J., Arnold, L., Moretti, S., Schmitt, M., Oleynik, S., Jaccard, S. L., Haug, G.H., 2020. Southern Ocean upwelling, Earth's obliquity, and glacial-interglacial atmospheric CO_2 change. Science 370 (6522), 1348–1352. https://doi.org/10.1126/science.abd2115.

Ai, X.E., Thöle, L.M., Auderset, A., Schmitt, M., Moretti, S., Studer, A.S., Michel, E., Wegmann, M., Mazaud, A., Bijl, P.K., Sigman, D.M., Martínez-García, A., Jaccard, S. L., 2024. The southward migration of the Antarctic Circumpolar current enhanced oceanic degassing of carbon dioxide during the last two deglaciations. Commun. Earth Environ. 5, 58. https://doi.org/10.1038/s43247-024-01216-x.

Anderson, R.F., Ali, S., Bradtmiller, L.I., Nielsen, S.H.H., Fleisher, M.Q., Anderson, B.E., Burckle, L.H., 2009. Wind-driven upwelling in the Southern Ocean and the deglacial rise in atmospheric CO_2. Science 323 (5920), 1443–1448. https://doi.org/10.1126/science.1167441.

Anderson, R.F., Sachs, J.P., Fleisher, M.Q., Allen, K.A., Yu, J., Koutavas, A., Jaccard, S.L., 2019. Deep-sea oxygen depletion and ocean carbon sequestration during the last ice age. Glob. Biogeochem. Cycles 33, 301–317. https://doi.org/10.1029/2018GB006049.

Bauska, T., Marcott, S.A., Brook, E.J., 2021. Abrupt changes in the global carbon cycle during the last glacial period. Nat. Geosci. 14, 91–96. https://doi.org/10.1038/s41561-020-00680-2.

Bereiter, B., Lüthi, D., Siegrist, M., Schüpbach, S., Stocker, T.F., Fischer, H., 2012. Mode change of millennial CO_2 variability during the last glacial cycle associated with a bipolar marine carbon seesaw. Proc. Natl. Acad. Sci. USA 109, 9755–9760. https://doi.org/10.1073/pnas.120406910.

Berger, A., Loutre, M.F., 1991. Insolation values for the climate of the last 10 million years. Quat. Sci. Rev. 10, 297–317. https://doi.org/10.1016/0277-3791(91)90033-Q.

Bradtmiller, L.I., Anderson, R.F., Sachs, J.P., Fleisher, M.Q., 2010. A deeper respired carbon pool in the glacial equatorial Pacific Ocean. Earth Planet. Sci. Lett. 299, 417–425. https://doi.org/10.1016/j.epsl.2010.09.022.

Broecker, W.S., McGee, D., 2013. The ^{13}C record for atmospheric CO_2: what is it trying to tell us? Earth Planet. Sci. Lett. 368, 175–182. https://doi.org/10.1016/j.epsl.2013.02.029.

Broecker, W.S., Barker, S., Clark, E., Hajdas, I., Bonani, G., Stott, L., 2004. Ventilation of glcail deep Pacific Ocean. Science 306 (5699), 1169–1172. https://doi.org/10.1126/science.1102293.

Burke, A., Robinson, L.F., 2012. The Southern Ocean's role in carbon exchange during the last deglaciation. Science 335 (6068), 557–561. https://doi.org/10.1126/science.1208163.

Calvert, S.E., Pedersen, T.F., 1993. Geochemistry of recent oxic and anoxic marine-sediments-implications for the geological record. Mar. Geol. 113 (1–2), 67–88. https://doi.org/10.1016/0025-3227(93)90150-T.

Calvert, S.E., Pedersen, T.F., 1996. Sedimentary geochemistry of manganese: Implications for the environment of formation of manganiferous black shales. Econ. Geol. 91 (1), 36–47. https://doi.org/10.2113/gsecongeo.91.1.36.

Carter, S.C., Griffith, E.M., Penman, D.E., 2016. Peak intervals of equatorial Pacific export production during the middle Miocene climate transition. Geology 44, 923–926. https://doi.org/10.1130/G38290.1.

Chen, M., Li, Q., Zhang, L., Zheng, F., Lu, J., Xiang, R., Zhang, L., Yan, W., Chen, Z., Xiao, S., 2008. Systematic biotic responses to palaeoenvironmental change in the late Pleistocene southern South China Sea: a preliminary study. J. Quat. Sci. 23 (8), 803–815. https://doi.org/10.1002/jqs.1178.

Clementi, V.J., Sikes, E.L., 2017. Southwest Pacific vertical structure influences on oceanic carbon storage since the last Glacial Maximum. Paleoceanogr. Pleoclimatol. 34, 734–754. https://doi.org/10.1029/2018PA003501.

Cliff, E., Khatiwala, S., Schmittner, A., 2021. Glacial deep ocean deoxygenation driven by biologically mediated air-sea disequilibrium. Nat. Geosci. 14, 43–50. https://doi.org/10.1038/s41561-020-00667-z.

Costa, K.M., McMamus, J.F., Anderson, R.F., Ren, H., Sigman, D.M., Winckler, G., Fleisher, M.Q., Marcantonio, F., Ravelo, A.C., 2016. No iron fertilization in the equatorial Pacific Ocean during the last ice age. Nature 529, 519–522. https://doi.org/10.1038/nature16453.

Costa, K.M., Anderson, R.F., McCanus, J.F., Winckler, G., Middleton, J.L., Langmuir, C. H., 2018. Trace element (Mn, Zn, Ni, V) and authigenic uranium (aU) geochemistry reveal sedimentary redox history on the Juan de Fuca Ridge, North Pacific Ocean. Geochim. Cosmochim. Acta 236, 79–98. https://doi.org/10.1016/j.gca.2018.02.016.

Crusius, J., Thomson, J., 2000. Comparative behavior of authigenic Re, U and Mo during reoxidation and subsequent long-term burial in marine sediments. Geochim. Cosmochim. Acta 64 (113), 2233–2242. https://doi.org/10.1016/S0016-7037(99)00433-0.

Dai, Y., Yu, J., Ren, H., Ji, X., 2022. Deglacial Subantarctic CO_2 outgassing driven by a weakened solubility pump. Nat. Commun. 13, 5193. https://doi.org/10.1038/s41467-022-32895-9.

de la Fuente, M., Skinner, L., Calvo, E., Pelejero, C., Cacho, I., 2015. Increased reservoir ages and poorly ventilated deep waters inferred in the glacial Eastern Equatorial Pacific. Nat. Commun. 6, 7420. https://doi.org/10.1038/ncomms8420.

Du, J., Haley, B.A., Mix, A.C., 2016. Neodymium isotopes in authigenic phases, bottom waters and detrital sediments in the Gulf of Alaska and their implications for paleocirculation reconstruction. Geochim. Cosmochim. Acta 193, 14–35. https://doi.org/10.1016/j.gca.2016.08.005.

Du, J., Haley, B.A., Mix, A.C., Walczak, M.H., Praetorius, S.K., 2018. Flushing of the deep Pacific Ocean and the deglacial rise of atmospheric CO_2 concentrations. Nat. Geosci. 11, 749–755. https://doi.org/10.1038/s41561-018-0205-6.

Duplessy, J.C., Shackleton, N.J., Matthews, R.K., Prell, W., Ruddiman, W.F., Caralp, M., Hendy, C.H., 1984. ^{13}C record of benthic foraminifera in the last interglacial ocean: Implications for the carbon cycle and the global deep water circulation. Quat. Res. 21 (2), 225–243. https://doi.org/10.1016/0033-5894(84)90099-1.

Durand, A., Chase, Z., Noble, T.L., Bostock, H., Jaccard, S.L., Townsend, A.T., Bindoff, N. L., Neil, H., Jacobsen, G., 2018. Reduced oxygenation at intermediate depths of the Southwest Pacific during the last glacial maximum. Earth Planet. Sci. Lett. 491, 48–57. https://doi.org/10.1016/j.epsl.2018.03.036.

Eggleston, S., Galbraith, E.D., 2018. The devil's in the disequilibrium: Multi-component analysis of dissolved carbon and oxygen changes under a broad range of forcings in a general circulation model. Biogeosciences 15 (12), 3761–3777. https://doi.org/10.5194/bg-15-3761-2018.

Elderfield, H., Ferretti, P., Greaves, M., Crowhurst, S., McCave, I.N., Hodell, D., Piotrowski, A.M., 2012. Evolution of ocean temperature and ice volume through the Mid-Pleistocene climate transition. Science 337 (6095), 704–709. https://doi.org/10.1126/science.1221294.

Ferrari, R., Jansen, M.F., Adkins, J.F., Burke, A., Stewart, A.L., Thompson, A.F., 2014. Antarctic Sea ice control on ocean circulation in present and glacial climates. Proc. Natl. Acad. Sci. USA 111, 8753–8758. https://doi.org/10.1073/pnas.132392211.

Francois, R., Honjo, S., Manganini, S.J., Ravizza, G.E., 1995. Biogenic barium fluxes to the deep sea: implications for paleoproductivity reconstruction. Glob. Biogeochem. Cycles 9 (2), 289–303. https://doi.org/10.1029/95GB00021.

Galbraith, E.D., Skinner, L.C., 2020. The biological pump during the last glacial maximum. Annu. Rev. Mar. Sci. 12, 559–586. https://doi.org/10.1146/annurev-marine-010419-010906.

Goldberg, E.D., Arrhenius, G.O.S., 1958. Chemistry of Pacific pelagic sediments. Geochim. Cosmochim. Acta 13 (2–3), 153–212. https://doi.org/10.1016/0016-7037(58)90046-2.

Gong, X., Lembke-Jene, L., Lohmann, G., Knorr, G., Tiedemann, R., Zou, J.J., Shi, X.F., 2019. Enhanced North Pacific deep-ocean stratification by stronger intermediate water formation during Heinrich Stadial 1. Nat. Commun. 10, 656.

Gottschalk, J., Riveiros, N.V., Waelbroeck, C., Skinner, L.C., Michel, E., Duplessy, J.-C., Hodell, D., Mackensen, A., 2016a. Carbon isotope offsets between benthic foraminifer species of the genus *Cibicides* (*Cibicidoides*) in the glacial sub-Antarctic Atlantic. Paleoceanography 31. https://doi.org/10.1002/2016PA003029.

Gottschalk, J., Skinner, L.C., Lippold, J., Vogel, H., Frank, N., Jaccard, S.L., Waelbroeck, C., 2016b. Biological and physical controls in the Southern Ocean on past millennial-scale atmospheric CO_2 changes. Nat. Commun. 7, 11539. https://doi.org/10.1038/ncomms11539.

Gray, W.R., Rae, J.W.B., Wills, R.C.J., Shevenell, A.E., Taylor, B., Burke, A., Foster, G.L., Lear, C.H., 2018. Deglacial upwelling, productivity and CO_2 outgassing in the North Pacific Ocean. Nat. Geosci. 11, 340–344. https://doi.org/10.1038/s41561-018-0108-6.

Hall, I.R., McCave, I.N., Shackleton, N.J., Weedon, G.P., Harris, S.E., 2001. Intensified deep Pacific inflow and ventilation in Pleistocene glacial times. Nature 412, 809–812. https://doi.org/10.1038/35090552.

Hawco, N.J., Ohnemus, D.C., Resing, J.A., Twining, B.S., Saito, M.A., 2016. A dissolved cobalt plume in the oxygen minimum zone of the eastern tropical South Pacific. Biogeosciences 13, 5697–5717. https://doi.org/10.5194/bg-13-5697-2016.

Hodell, D.A., Venz, K.A., Charles, C.D., Ninnemann, U.S., 2003. Pleistocene vertical carbon isotope and carbonate gradients in the South Atlantic sector of the Southern Ocean. Geochem. Geophys. Geosyst. 4, 1–19. https://doi.org/10.1029/2002GC000367.

Holzer, M., DeVries, T., de Lavergne, C., 2021. Diffusion controls the ventilation of a Pacific Shadow Zone above abyssal overturning. Nat. Commun. 12, 4348. https://doi.org/10.1038/s41467-021-24648-x.

Hu, R., Piotrowski, A.M., 2018. Neodymium isotope evidence for glacial-interglacial variability of Deepwater transit time in the Pacific Ocean. Nat. Commun. 9, 4709. https://doi.org/10.1038/s41467-018-07079-z.

Hu, R., Bostock, H.C., Gottschalk, J., Piotrowski, A.M., 2023. Reconstructing Ocean oxygenation changes from U/Ca and U/Mn in foraminiferal coatings: Proxy validation and constraints on glacial oxygenation changes. Quat. Sci. Rev. 306, 108028. https://doi.org/10.1016/j.quascirev.2023.108028.

Jaccard, S.L., Haug, G.H., Sigman, D.M., Pedersen, T.F., Thierstein, H.R., Rohl, U., 2005. Glacial/interglacial changes in subarctic North Pacific stratification. Science 308, 1003–1006. https://doi.org/10.1126/science.11086.

Jaccard, S.L., Galbraith, E.D., Sigman, D.M., Haug, G.H., Francois, R., Pedersen, T.F., 2009. Subarctic Pacific evidence for a glacial deepening of the oceanic respired carbon pool. Earth Planet. Sci. Lett. 277, 156–165. https://doi.org/10.1016/j.epsl.2008.10.017.

Jaccard, S.L., Hayes, C.T., Martinez-Garcia, A., Hodell, D.A., Anderson, R.F., Sigman, D. M., Haug, G.H., 2013. Two modes of change in Southern Ocean productivity over the past million years. Science 339, 1419–1423. https://doi.org/10.1126/science.1227545.

Huang, H., Gutjahr, M., Eisenhauer, A., Kuhn, G., 2020. No detectable Weddell Sea Antarctic Bottom Water export during the Last and Penultimate Glacial Maximum. Nat. Commun. 11, 424.

Jaccard, S.L., Galbraith, E.D., Martinez-Garcia, A., Anderson, R.F., 2016. Covariation of deep Southern Ocean oxygenation and atmospheric CO_2 through the last ice age. Nature 530, 207–210. https://doi.org/10.1038/nature16514.

Jacobel, A.W., McManus, J.F., Anderson, R.F., Winckler, G., 2017. Repeated storage of respired carbon in the equatorial Pacific Ocean over the last three glacial cycles. Nat. Commun. 8, 1727. https://doi.org/10.1038/s41467-017-01938-x.

Jacobel, A.W., Anderson, R.F., Jaccard, S.L., McManus, J.F., Pavia, F.J., Winckler, G., 2020. Deep Pacific storage of respired carbon during the last ice age: perspectives from bottom water oxygen reconstructions. Quat. Sci. Rev. 230, 106065. https://doi.org/10.1016/j.quascirev.2019.106065.

Jansen, M.F., 2016. Glacial ocean circulation and stratification explained by reduced atmospheric temperature. Proc. Natl. Acad. Sci. USA 114, 45–50. https://doi.org/10.1073/pnas.1610438113.

Jansen, M.F., Nadeau, L.-P., 2016. The effect of Southern Ocean surface buoyancy loss on the deep-ocean circulation and stratification. J. Phys. Oceanogr. 46, 3455–3470. https://doi.org/10.1175/JPO-D-16-0084.1.

Kawabe, M., Fujio, S., 2010. Pacific Ocean circulation based on observation. J. Oceanogr. 66, 389–403. https://doi.org/10.1007/s10872-010-0034-8.

Key, R.M., Kozyr, A., Sabine, C.L., Lee, K., Wanninkhof, R., Bullister, J.L., Feely, R.A., Millero, F.J., Mordy, C., Peng, T.-H., 2004. A global ocean carbon climatology: results from Global Data Analysis Project (GLODAP). Glob. Biogeochem. Cycles 18, GB4031. https://doi.org/10.1029/2004GB002247.

Khatiwala, S., Schmittner, A., Muglia, J., 2019. Air-sea disequilibrium enhances ocean carbon storage during glacial periods. Sci. Adv. 5, eaaw4981. https://doi.org/10.1126/sciadv.aaw4981.

Kumar, N., Anderson, R.F., Mortlock, R.A., Froelich, P.N., Kubik, P., Dittrich-Dittrich-Hannen, B., Suter, M., 1995. Increased biological productivity and export production in the glacial Southern Ocean. Nature 378, 675–680. https://doi.org/10.1038/378675a0.

Li, G., Rashid, H., Zhong, L., Xu, X., Yan, W., Chen, Z., 2018. Changes in deep water oxygenation of the South China Sea since the last glacial period. Geophys. Res. Lett. 45, 9058–9066. https://doi.org/10.1029/2018GL078568.

Lisiecki, L.E., 2010. A simple mixing explanation for late Pleistocene changes in the Pacific-South Atlantic benthic $\delta^{13}C$ gradient. Clim. Past 6, 305–314. https://doi.org/10.5194/cp-6-305-2010.

Loveley, M.R., Marcantonio, F., Wisler, M.M., Hertzberg, J.E., Schmidt, M.W., Lyle, M., 2017. Millennial-scale iron fertilization of the eastern equatorial Pacific over the past 100,000 years. Nat. Geosci. 10 (10), 760–764. https://doi.org/10.1038/ngeo3024.

Lu, J., Chen, G., Frierson, D.M.W., 2010. The position of the midlatitude storm track and eddy-driven westerlies in Aquaplanet AGCMs. J. Atmos. Sci. 67, 3984–4000. https://doi.org/10.1175/2010JAS3477.1.

Lynch-Stieglitz, J., Stocker, T.F., Broecker, W.S., Fairbanks, G., 1995. The influence of air-sea exchange on the isotopic composition of oceanic carbon: observations and modeling. Glob. Biogeochem. Cycles 9 (4), 653–665. https://doi.org/10.1029/95GB02574.

Mackensen, A., 2012. Strong thermodynamic imprint on recent bottom-water and epibenthic $\delta^{13}C$ in the Weddell Sea revealed: Implications for glacial Southern Ocean ventilation. Earth Planet. Sci. Lett. 317-318, 20–26. https://doi.org/10.1016/j.epsl.2011.11.030.

Mangini, A., Jung, M., Laukenmann, S., 2001. What do we learn from peaks of uranium and of manganese in deep sea sediments? Mar. Geol. 177, 63–78. https://doi.org/10.1016/S0025-3227(01)00124-4.

Marcantonio, F., Hostak, R., Hertzberg, J.E., Schmidt, M.W., 2020. Deep Equatorial Pacific Ocean oxygenation and atmospheric CO_2 over the last ice age. Sci. Rep. 10, 6606. https://doi.org/10.1038/s41598-020-63628-x.

Marcott, S.A., Bauska, T.K., Buizert, C., Steig, E.J., Rosen, J.L., Cuffey, K.M., Fudge, T.J., Severinghaus, J.P., Ahn, J., Kalk, M.L., McConnell, J.R., Sowers, T., Taylor, K.C., White, J.M.C., Brook, E.J., 2014. Centennial-scale changes in the global carbon cycle during the last deglaciation. Nature 514, 616–619. https://doi.org/10.1038/nature13799.

Martínez-Botí, M.A., Marino, G., Foster, G.L., Ziveri, P., Henehan, M.J., Rae, J.W.B., Mortyn, P.G., Vance, D., 2015. Boron isotope evidence for oceanic carbon dioxide leakage during the last deglaciation. Nature 518, 219–222. https://doi.org/10.1038/nature14155.

Martínez-García, A., Sigman, D.M., Ren, H., Anderson, R.F., Straub, M., Hodell, D.A., Jaccard, S.L., Eglinton, T.I., Haug, G.H., 2014. Iron fertilization of the Subantarctic Ocean during the last ice age. Science 343 (6177), 1347–1350. https://doi.org/10.1126/science.1246848.

Matsumoto, K., Oba, T., Lynch-Stieglitz, J., Yamamoto, H., 2002. Interior hydrography and circulation of the glacial Pacific Ocean. Quat. Sci. Rev. 21, 1693–1704. https://doi.org/10.1016/S0277-3791(01)00142-1.

McCave, I.N., Carter, L., Hall, I.R., 2008. Glacial-interglacial changes in water mass structure and flow in the SW Pacific Ocean. Quat. Sci. Rev. 27, 1886–1908. https://doi.org/10.1016/j.quascirev.2008.07.010.

McManus, J., Berelson, W.M., Klinkhammer, G.P., Hammond, D.E., Holm, C., 2005. Authigenic uranium: Relationship to oxygen penetration depth and organic carbon rain. Geochim. Cosmochim. Acta 69 (1), 95–108. https://doi.org/10.1016/j.gca.2004.06.023.

Menviel, L., Mouchet, A., Meissner, K.J., Joos, F., England, M.H., 2015. Impact of oceanic circulation changes on atmospheric $\delta^{13}CO_2$. Glob. Biogeochem. Cycles 29, 1944–1961. https://doi.org/10.1002/2015GB005207.

Menviel, L., Yu, J., Joos, F., Mouchet, A., Meissner, K.J., England, M.H., 2017. Poorly ventilated deep ocean at the last Glacial Maximum inferred from carbon isotopes: a data-model comparison study. Paleoceanography 32, 2–17. https://doi.org/10.1002/2016PA003024.

Menviel, L., Spence, P., Yu, J., Chamberlain, M.A., Matear, R.J., Meissner, K.J., England, M.H., 2018. Southern Hemisphere westerlies as a driver of the early deglacial atmospheric CO_2 rise. Nat. Commun. 9, 2503. https://doi.org/10.1038/s41467-018-04876-4.

Morford, J.L., Emerson, S., 1999. The geochemistry of redox sensitive trace metals in sediments. Geochim. Cosmochim. Acta 63 (11−12), 1735–1750. https://doi.org/10.1016/s0016-7037(99)00126-x.

Nameroff, T.J., Balistrieri, L.S., Murray, J.W., 2002. Suboxic trace metal geochemistry in the Eastern Tropical North Pacific. Geochim. Cosmochim. Acta 66, 1139–1158. https://doi.org/10.1016/S0016-7037(01)00843-2.

Nan, J., Tsang, M.-Y., Li, J., Köster, M., Henkel, S., Lin, F., Yao, W., 2023. Postdepositional behavior of molybdenum in deep sediments and implications for paleoredox reconstruction. Geophys. Res. Lett. 50, e2023GL104706. https://doi.org/10.1029/2023GL104706.

Oka, A., Niwa, Y., 2013. Pacific deep circulation and ventilation controlled by tidal mixing away from the sea bottom. Nat. Commun. 4, 2419. https://doi.org/10.1038/ncomms3419.

Party, Shipboard Scientific, 2000. Site 1143. In: Wang, P., Prell, W.L., Blum, P., Rea, D. K., Clemens, S.C. (Eds.), Proceedings of the Ocean Drilling Program, Initial Reports, 184. Ocean Drilling Program, College Station, Texas, pp. 1–103. https://doi.org/10.2973/odp.proc.ir.184.104.2000.

Paytan, A., Kastner, M., 1996. Benthic Ba fluxes in the central Equatorial Pacific, implications for the oceanic Ba cycle. Earth Planet. Sci. Lett. 142, 439–450. https://doi.org/10.1016/0012-821X(96)00120-3.

Paytan, A., Kastner, M., Chavez, F.P., 1996. Glacial to interglacial fluctuations in productivity in the equatorial Pacific as indicated by marine barite. Science 274, 1355–1357. https://doi.org/10.1126/science.274.5291.1355.

Peterson, C.D., Lisiecki, L.E., Stern, J.V., 2014. Deglacial whole-ocean $\delta^{13}C$ change estimated from 480 benthic foraminiferal records. Paleoceanography 29, 549–563. https://doi.org/10.1002/2013PA002552.

Qu, T., Girton, J.B., Whitehead, J.A., 2006. Deepwater overflow through Luzon Strait. J. Geophys. Res. Oceans 111, C01002. https://doi.org/10.1029/2005jc003139.
Rae, J.W.B., Sarnthein, M., Foster, G.L., Ridgwell, A., Grootes, P.M., Elliott, T., 2014. Deep water formation in the North Pacific and deglacial CO_2 rise. Paleoceanography 29, 645–667. https://doi.org/10.1002/2013PA002570.
Rae, J.W.B., Burke, A., Robinson, L.F., Adkins, J.F., Chen, T., Cole, C., Greenop, R., Li, T., Littley, E.F.M., Nita, D.C., Stewart, J.A., Taylor, B.J., 2018. CO_2 storage and release in the deep Southern Ocean on millennial to centennial timescales. Nature 562, 569–573. https://doi.org/10.1038/s41586-018-0614-0.
Rafter, P.A., Gray, W.R., Hines, S.K.V., Burke, A., Costa, K.M., Gottschalk, J., Hain, M.P., Rae, J.W.B., Southon, J.R., Walczak, M.H., Yu, J., Adkins, J.F., Devries, T., 2022. Global reorganization of deep-sea circulation and carbon storage after the last ice age. Sci. Adv. 8, eabq5434. https://doi.org/10.1126/sciadv.abq5434.
Ronge, T.A., Steph, S., Tiedemann, R., Prange, M., Merkel, U., Nürnberg, D., Kuhn, G., 2015. Pushing the boundaries: Glacial/interglacial variability of intermediate and deep waters in the Southwest Pacific over the last 350,000 years. Paleoceanography 30, 23–38. https://doi.org/10.1002/2014PA002727.
Ronge, T.A., Tiedemann, R., Lamy, F., Köhler, P., Alloway, B.V., Pol-Holz, R.D., Pahnke, K., Southon, J., Wacker, L., 2016. Radiocarbon constraints on the extent and evolution of the South Pacific glacial carbon pool. Nat. Commun. 7, 11487. https://doi.org/10.1038/ncomms11487.
Sachs, J.P., Anderson, R.F., Lehman, S.J., 2001. Glacial surface temperatures of the Southeast Atlantic Ocean. Science 293, 2077–2079. https://doi.org/10.1126/science.1063584.
Schlitzer, R., 2022. Ocean Data View. https://odv.awi.de.
Schmittner, A., Gruber, N., Mix, A.C., Key, R.M., Tagliabue, A., Westberry, T.K., 2013. Biology and air-sea gas exchange controls on the distribution of carbon isotope ($\delta^{13}C$) in the ocean. Biogeosciences 10, 5793–5816. https://doi.org/10.5194/bg-10-5793-2013.
Schoepfer, S.D., Shen, J., Wei, H., Tyson, R.V., Ingall, E., Algeo, T.J., 2015. Total organic carbon, organic phosphorus, and biogenic barium fluxes as proxies for paleomarine productivity. Earth Sci. Rev. 149, 23–52. https://doi.org/10.1016/j.earscirev.2014.08.017.
Shaw, T.J., Gieskes, J.M., Jahnke, R.A., 1990. Early diagenesis in differing depositional environments: the response of transition metals in pore water. Geochim. Cosmochim. Acta 54 (5), 1233–1246. https://doi.org/10.1016/0016-7037(90)90149-F.
Sigman, D.M., Boyle, E.A., 2000. Glacial/interglacial variations in atmospheric carbon dioxide. Nature 407, 859–869. https://doi.org/10.1038/35038000.
Sigman, D.M., Hain, M.P., Haug, G.H., 2010. The polar ocean and glacial cycles in atmospheric CO_2 concentration. Nature 466, 47–55. https://doi.org/10.1038/nature09149.
Sikes, E.L., Elmore, A.C., Cook, M.S., Allen, K.A., Guilderson, T.P., 2016. Glacial water mass structure and rapide $\delta^{18}O$ and $\delta^{13}C$ changes during the last glacial termination in the Southwest Pacific. Earth Planet. Sci. Lett. 456, 87–97. https://doi.org/10.1016/j.epsl.2016.09.043.
Sikes, E.L., Allen, K.A., Lund, D.C., 2017. Enhanced $\delta^{13}C$ and $\delta^{18}O$ differences between the South Atlantic and South Pacific during the last glaciation: the deep gateway hypothesis. Paleoceanography 32, 1000–1017. https://doi.org/10.1002/2017pa003118.
Sikes, E.L., Umling, N.E., Allen, K.A., Ninnemann, U.S., Robinson, R.S., Russell, J.L., Willianms, T.J., 2023. Southern Ocean glacial conditions and their influence on deglacial events. Nat. Rev. Earth Environ. 4, 454–470. https://doi.org/10.1038/s43017-023-00436-7.
Skinner, L., Fallon, S., Waelbroeck, C., Michel, E., Barker, S., 2010. Ventilation of the Deep Southern Ocean and Deglacial CO_2 rise. Science 328 (5982), 1147–1151. https://doi.org/10.1126/science.1183627.
Stephens, B.B., Keeling, R.F., 2000. The influence of Antarctic Sea ice on glacial-interglacial CO_2 variations. Nature 404, 171–174. https://doi.org/10.1038/35004556.
Stewart, A., 2017. Mixed up at the sea floor. Nature 551, 178–179. https://doi.org/10.1038/551178b.
Stott, L.D., Shao, J., Yu, J., Harazin, K.M., 2021. Evaluating the glacial-deglacial carbon respiration and ventilation change hypothesis as a mechanism for changing atmospheric CO_2. Geophys. Res. Lett. 48, e2020GL091296. https://doi.org/10.1029/2020GL091296.
Talley, L.D., 2013. Closure of the global overturning circulation through the Indian, Pacific, and southern oceans: schematics and transports. Oceanography 26 (1), 80–97. https://doi.org/10.5670/oceanog.2013.07.
Taylor, S.R., Mclennan, S.M., 1985. The Continental Crust: Its Composition and Evolution. Blackwell Scientific, Oxford.
Thiagarajan, N., McManus, J.F., 2019. Productivity and sediment focusing in the Eastern Equatorial Pacific during the last 30,000 years. Deep Sea Res. I 147, 100–110. https://doi.org/10.1016/j.dsr.2019.03.007.
Timmermann, A., Friedrich, T., Timm, O.E., Chikamoto, M.O., Abe-Ouchi, A., Ganopolski, A., 2014. Modeling obliquity and CO_2 effects on Southern Hemisphere climate during the past 408 ka. J. Clim. 27, 1863–1875. https://doi.org/10.1175/JCLI-D-13-00311.1.
Tribovillard, N., Algeo, T.J., Lyons, T., Riboulleau, A., 2006. Trace metals as paleoredox and paleoproductivity proxies: an update. Chem. Geol. 232, 12–32. https://doi.org/10.1016/j.chemgeo.2006.02.012.
Wan, S., Jian, Z., Gong, X., Dang, H., Wu, J., Qiao, P., 2020. Deep water [CO2-3] and circulation in the South China Sea over the last glacial cycle. Quat. Sci. Rev. 243, 106499. https://doi.org/10.1016/j.quascirev.2020.106499.
Wang, G., Xie, S.-P., Qu, T., Huang, R.X., 2011. Deep South China Sea circulation. Geophys. Res. Lett. 38, L05601. https://doi.org/10.1029/2010gl046626.
Warren, B.A., 1983. Why is no deep water formed in the North Pacific? J. Mar. Res. 41 (2), 327–347. https://doi.org/10.1357/002224083788520207.
Wei, G., Gui, X., Li, X., Chen, Y., Yu, J., 2000. Strontium and neodymium isotopic compositions of detrital sediment of NS90-103 from South China Sea: Variations and their paleoclimate implication. Sci. China Ser. D Earth Sci. 43 (6), 596–604. https://doi.org/10.1007/bf02879503.
Wei, G., Liu, Y., Li, X., Chen, M., Wie, W., 2003. High-resolution elemental records from the South China Sea and their paleoproductivity implications. Paleoceanography 18 (2), 1054. https://doi.org/10.1029/2002pa000826.
Whittaker, T.E., Hendy, C.H., Hellstrom, J.C., 2011. Abrupt millennial-scale changes in intensity of Southern Hemisphere westerly winds during marine isotope stages 2-4. Geology 39, 455–458. https://doi.org/10.1130/G31827.1.
Winckler, G., Anderson, R.F., Jaccard, S.L., Marcantonio, F., 2016. Ocean dynamics, not dust, have controlled equatorial Pacific productivity over the past 500,000 years. Proc. Natl. Acad. Sci. USA 113, 6119–6124. https://doi.org/10.1073/pnas.1600616113.
Wu, Q., Colin, C., Liu, Z., Douville, E., Dubois-Dauphin, Q., Frank, N., 2015. New insights into hydrological exchange between the South China Sea and the Western Pacific Ocean based on the Nd isotopic composition of seawater. Deep-Sea Res. II 122, 25–40. https://doi.org/10.1016/j.dsr2.2015.11.005.
Yao, W., Griffith, E., Paytan, A., 2021. Pelagic Barite: Tracer of Ocean Productivity and a Recorder of Isotopic Compositions of Seawater S, O, Sr, Ca and Ba. Cambridge University Press, Cambridge.
Yu, J., Broecker, W., Elderfield, H., Jin, Z., McManus, J., Zhang, F., 2010. Loss of carbon from the deep sea since the last Glacial Maximum. Science 330, 1084–1087. https://doi.org/10.1126/science.1193221.
Yu, J., Anderson, R.F., Jin, Z., Rae, J.W.B., Opdyke, B.N., Eggins, S.M., 2013. Responses of the deep ocean carbonate system to carbon reorganization during the last Glacial-interglacial cycle. Quat. Sci. Rev. 76, 39–52. https://doi.org/10.1016/j.quascirev.2013.06.020.
Yu, J., Anderson, R.F., Jin, Z., Menviel, L., Zhang, F., Ryerson, F.J., Rohling, E.J., 2014. Deep South Atlantic carbonate chemistry and increased interocean deep water exchange during last deglaciation. Quat. Sci. Rev. 90, 80–89. https://doi.org/10.1016/j.quascirev.2014.02.018.
Yu, J., Menviel, L., Jin, Z.D., Anderson, R.F., Jian, Z., Piotrowski, A.M., Ma, X., Rohling, E.J., Zhang, F., Marino, G., McManus, J.F., 2020. Last glacial atmospheric CO_2 decline due to widespread Pacific deep-water expansion. Nat. Geosci. 13, 628–633. https://doi.org/10.1038/s41561-020-0610-5.
Yu, J., Anderson, R.F., Jin, Z.D., Ji, X., Thornalley, J.R., Wu, L., Thouveny, N., Cai, Y., Tan, L., Zhang, F., Menviel, L., Tian, J., Xie, X., Rohling, E.J., McManus, J.F., 2023. Millennial atmospheric CO_2 changes linked to ocean ventilation modes over past 150,000 years. Nat. Geosci. 16, 1166–1173. https://doi.org/10.1038/s41561-023-01297-x.
Zheng, Y., Anderson, R.F., van Geen, A., Fleisher, M.Q., 2002. Remobilization of authigenic uranium in marine sediments by bioturbation. Geochim. Cosmochim. Acta 66, 1759–1772. https://doi.org/10.1016/S0016-7037(01)00886-9.
Zhong, Y., Wilson, D.J., Liu, J., Wan, S., Bao, R., Liu, J., Zhang, Y., Wang, X., Liu, Y., Liu, X., Zhao, Y., Li, S., Liu, Q., 2021. Contrasting sensitivity of weathering proxies to quaternary climate and sea-level fluctuations on the southern slope of the South China Sea. Geophys. Res. Lett. 48 (24), e2021GL096433. https://doi.org/10.1029/2021GL096433.
Zou, J., Shi, X., Zhu, A., Kandasamy, S., Gong, X., Lembke-Jene, L., Chen, M.-T., Wu, Y., Ge, S., Liu, Y., Xue, X., Lohmann, G., Tiedemann, R., 2020. Millennial-scale variations in sedimentary oxygenation in the western subtropical North Pacific and its links to North Atlantic climate. Clim. Past 16, 387–407. https://doi.org/10.5194/cp-16-387-2020.